PHYSICAL REVIEW B VOLUME 27, NUMBER 9 1 MAY 1983

Combined effects of exchange and g-value anisotropy in the conduction-electron spin resonance of metals

Robert H. Silsbee
Department of Physics, Cornell University, Ithaca, New York 14853

James P. Long
Naval Research Laboratory, Washington, D.C. 20375
(Received 30 August 1982)

A heuristic model is developed to explore the combined effects of exchange and g-value anisotropy in the conduction-electron spin resonance in polyvalent metals where it may be appropriate to consider the electrons in different Brillouin zones to be partially decoupled from one another. Within the framework of this model the resonance should show structure at low temperature, and the conventional analysis of resonance data, using the theory of Platzman and Wolff to obtain the exchange parameter B_0, can be substantially in error if the effects of g-value anisotropy are not properly accounted for. Some features of existing data for aluminum are discussed in the context of this model, and it is noted that spin-resonance results may be able to remove the current ambiguity in the sign of the pseudopotential matrix element V_{111} used in calculations of the band structure of aluminum.

I. INTRODUCTION

The role of g-value anisotropy, the dependence of the conduction-electron g value upon position on the Fermi surface, in determining the experimentally measured spectrum of conduction-electron spin resonance (CESR) in metals has not been extensively explored. Typically, the momentum scattering time for electrons is sufficiently short that this g-value anisotropy is motionally averaged and contributes principally only to the width of the observed resonance.[1] In very pure materials at low temperature, however, the scattering time may become sufficiently long to require a more detailed examination of the effects of g-value anisotropy. Also, if there is significant exchange interaction among the conduction electrons the combined effects of exchange and motional averaging of the g-value anisotropy must be considered.

Freedman and Fredkin[2] (FF) have given a most useful discussion of the general problem of the effects of g-value anisotropy in the presence of exchange. Two of their principal results are expressions for the linewidth and g-value shift as a function of the momentum scattering time valid throughout the range from narrowing by exchange, at low temperature, to narrowing by momentum scattering at high temperature. They also note, in agreement with Kaplan and Glasser,[3] that the effect of exchange, with isotropic g, in giving a complex diffusion constant for magnetization can be simulated by the presence of g-value anisotropy without exchange. Walker[4] and later Montgomery[4] have also explored the consequences of the combined effects of g-value anisotropy and exchange using specific models for the g-value anisotropy.

The explicit results of FF in the presence of both g-value anisotropy and exchange, used extensively in the interpretation of CESR results in aluminum,[5-7] rely on the assumption that the rms spread in g values over the Fermi surface is small compared to the exchange parameter, i.e., $\langle(\delta g/g)^2\rangle^{1/2} \ll B_0$. Results of $\delta g(k)$ calculations by Beuneu[7] show that the simple explicit results of FF must be used with caution. The g-value shifts, averaged over Landau orbits, show an rms g-value variation $\langle(\delta g/g)^2\rangle^{1/2} \sim 0.033$, uncomfortably close to the lower estimate of B_0 of 0.06 measured by Dunifer *et al.*[8] Further, the rms g-value variation, using point values rather than orbital averages, is 0.23, indicating the need for substantial care in choosing appropriate δg's to use in the FF formalism. Some important consequences of this g-value distribution have been pursued further in another publication[9] concerned with the regime in which motional narrowing by scattering, not exchange narrowing, determines the width of the resonance.

There is an additional feature of Beuneu's results, illustrated in Fig. 1, which suggests the use of the model discussed in detail later in this paper to probe

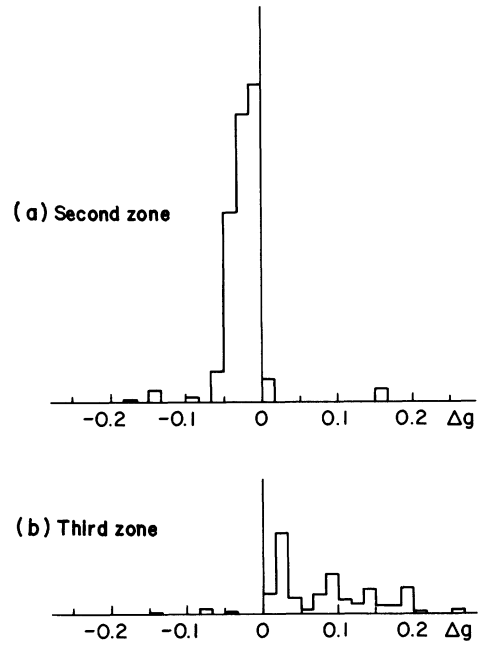

FIG. 1. Histogram of density of orbitally averaged g-value shifts, δg, for (a) the second zone and (b) the third zone in aluminum, from Ref. 7.

the consequences of g-value anisotropy. Figures 1(a) and 1(b) give, in histogram form, the distribution functions of the orbitally averaged g values for electrons on the pieces of the Fermi surface in the second and third zones, respectively. The second-zone electrons have a narrow distribution of g values with a mean shift of -0.023, while those of the third zone have a mean shift of $+0.078$ and about $3\times$ the spread.

It should be noted that the results of Beuneu are based on the Ashcroft model[10] for the aluminum band structure and the pseudopotential matrix element V_{111} has been assumed positive. In fact, there remains ambiguity in the sign of V_{111} since it enters the band-theory calculation only as V_{111}^2. Because the dominant g-value shifts in aluminum result from coupling across the V_{111} gaps, they are reversed in sign if the sign of V_{111} is reversed. Thus the possibility should be kept in mind that the sign of the $g-2$ axis of Fig. 1 could be reversed, and that the second-zone electrons could well have the positive g-value shift rather than the third-zone electrons. In principle, the CESR experiment is capable of removing this ambiguity in the sign of V_{111}.

In aluminum, with high enough purity and at sufficiently low temperatures, there will ultimately be neither impurities, nor phonons of adequate wave vector, to scatter electrons between the second and third zones, though scattering over the individual zones could still be effective in narrowing the individual zone g-value distributions illustrated in Fig. 1. This idea suggests a heuristic model for exploring the combined effects of g-value anisotropy and exchange, namely a model of two groups of spins, each with a characteristic g value, linewidth, and diffusivity, which are coupled by exchange and by interzone scattering. This is an idea already discussed briefly by Stesmans and Witters[11] with regard to CESR results in zinc and magnesium. This model will unlikely portray accurately the observed behavior of aluminum; it *will* highlight a number of important features which may be evidenced in the CESR of polyvalent metals. The formal equations describing this model are presented in Sec. II, and some experimental implications are discussed in Sec. III.

II. THEORETICAL FRAMEWORK

A. Model formulation

A model is desired which is both solvable and which reflects some of the important physics inherent in metallic systems with a wide spread in g values over the Fermi surface, systems for which the specific predictions of the Freedman-Fredkin theory may not be valid. The structure of the g-value distribution[7] indicated in Fig. 1, with the g-value shifts in the second zone narrowly centered at -0.023 and the broader distribution for the third zone centered at a shift of $+0.078$, suggest a phenomenological model treating two groups of spins. A straightforward generalization of the development of Platzman and Wolff[12] (PW) is possible with the simplifications outlined below. These simplifications are of course open to criticism, but the result does allow relatively simple solutions, and hence the model provides useful illustration of the kinds of physical behavior to be expected.

Two groups, $i=1,2$, of electrons are defined each described by a 2×2 density matrix $\rho_i(\vec{p},\vec{r},t)$. The trace of ρ_i gives the probability of finding an electron in the momentum state $\vec{p}$ at position $\vec{r}$, the difference in diagonal components gives the contribution of that state to the magnetization in the direction of spin quantization, and the off-diagonal components give the associated transverse magnetization. Generalizing the development of PW, coupled transport equations for the densities are written to describe the effect of a driving field

$$(\hat{x}H_x+\hat{y}H_y)\exp(i\vec{k}\cdot\vec{r}-i\omega t)$$

in the presence of a uniform steady magnetic field $\hat{z}H_0$. The steady-state equations are linearized in the circularly polarized driving field amplitude

$H_1 \equiv H_x + iH_y$, and the resonant components of the response amplitudes of the density matrices $\rho_i(\vec{p},\vec{r},t)$ are denoted by $\rho_i^+(\vec{p})$.

Related response amplitudes a_i and $\vec{b}_i$ are defined by the convenient ansatz

$$\rho_i^+(p)=(a_i+\vec{v}\cdot\vec{b}_i)\left[\frac{-\partial n^0}{\partial E}\right], \tag{1}$$

representing the leading two terms in an expansion, analogous to PW equation (58.17), of $\rho_i^+(\vec{p})$ in a set of functions defined over the Fermi surface. The term $(-\partial n^0/\partial E)$, with n^0 the Fermi distribution function, reflects the fact that the density matrix $\rho^+(\vec{p})$ is significantly perturbed only near the Fermi surface.

The amplitude a_i is essentially the resonant magnetization density m_i^+ associated with electron group i, since

$$\begin{aligned} m_i^+ &= \gamma_i \int \frac{d^3p}{8\pi^3}\rho^+(\vec{p}) \\ &= \gamma_i \int_{\text{Fermi surface}} d^2p \int \frac{dE}{|\vec{\nabla}_{\vec{p}}E(\vec{p})|} a_i \left[-\frac{\partial n^0}{\partial E}\right] \\ &= \gamma_i N_i(\epsilon_{Fi}) a_i \ . \end{aligned} \tag{2}$$

$N_i(\epsilon_{Fi})$ is the *single-spin* density of states at the Fermi energy ϵ_{Fi} for group i, γ_i is the gyromagnetic ratio for the ith group, and units have been defined to give $\hbar \equiv 1$. In a similar fashion, the vector amplitude $\vec{b}_i$ gives the magnetization current density

$$\vec{j}_i^{\,+} = \gamma_i \int \frac{d^3p}{8\pi^3}\vec{v}\rho^+(\vec{p}) = \gamma_i N_i(\epsilon_{Fi})\vec{b}_i/3 \ , \tag{3}$$

where the result for a spherical Fermi surface $\langle v_\alpha^2\rangle = v_F^2/3$ for $\alpha = x,y,z$ has been used.

The coupled transport equations for the amplitudes a_i (magnetization) and $\vec{b}_i$ (magnetization currents) involve the following properties of the two electron groups:

(i) resonant frequencies, in absence of exchange, equal to $\gamma_i H_0$ with H_0 the static applied field. Note that this γ is defined to be consistent with the usual convention in magnetic resonance, but differs by a factor of 2 from the PW development. It is convenient to introduce parameters $\gamma_0 \equiv (\gamma_1\gamma_2)^{1/2}$ and $\epsilon \equiv (\gamma_2-\gamma_1)/(\gamma_2+\gamma_1)$ in terms of which

$$\begin{aligned} \gamma_1 &= \gamma_0[(1-\epsilon)/(1+\epsilon)]^{1/2} \ , \\ \gamma_2 &= \gamma_0[(1+\epsilon)/(1-\epsilon)]^{1/2} \ . \end{aligned} \tag{4}$$

The results of Beuneu[7] correspond to $\epsilon = +0.025$ if $i=2$ is associated with the second-zone electrons, and $i=1$ with the third zone. Ambiguity in the sign of the crystal-field matrix element V_{111} implies an ambiguity in the sign of the calculated ϵ;

(ii) phenomenological spin-resonance widths $1/T_i$ (no distinction will be made between longitudinal and transverse relaxation times);

(iii) momentum scattering times τ_i' assumed isotropic;

(iv) spherical Fermi surfaces with Fermi velocities v_i and cyclotron resonance frequencies ω_{ci};

(v) exchange coupling parameters B_{ii} corresponding to the B_0 defined in PW (Ref. 12), Eq. (52.33); higher-order B's are assumed zero. The B_{ii}, as well as the B_{ij} introduced shortly, are directly related to the spin-dependent electron-electron interaction energy in the Landau Fermi-liquid theory. The spin-dependent interaction energy of an electron of momentum p in group i with an electron of moment p' in group j may be denoted

$$\epsilon_{ip,jp'} = \zeta_{ij}\vec{\sigma}_{ip}\cdot\vec{\sigma}_{jp'} \ , \tag{5a}$$

$$\zeta_{ij} = \zeta_{ji} \ , \tag{5b}$$

if the exchange is assumed independent of p and p'—one of many simplifications used in this paper. The uncoupled transport equations are more conveniently written in terms of the Landau parameters B_{ii}, defined by

$$B_{ij} \equiv N_j(\epsilon_{Fj})\zeta_{ij} \tag{6}$$

with $i=j$;

(vi) magnetic susceptibilities in absence of exchange χ_{0i}, used frequently as an expression of the single-spin density of states via

$$N(\epsilon_{Fi}) = \chi_{0i}/\gamma_i^2 \ . \tag{7}$$

The two groups of electrons are coupled by mutual exchange and by intergroup scattering. The cross exchange parameters B_{ij}, $i \neq j$, were defined already in the preceding paragraph as an obvious extension of the intragroup B's. Intergroup scattering, assumed independent of spin and momentum, is described by two parameters τ_{ij}, with τ_{ij}^{-1} being the probability per unit time that any particular electron in group j be scattered to the i group in the absence of restriction by the Pauli exclusion principle. The detailed balance condition, reflecting the fact that cross-scattering lifetimes will be shorter for electrons in the group with the lower density of states, receives quantitative expression in the relation

$$\frac{1}{\tau_{ij}}N_j(\epsilon_{Fj}) = \frac{1}{\tau_{ji}}N_i(\epsilon_{Fi}) \ . \tag{8}$$

It is convenient to introduce a parameter α to describe the relative densities of states at the Fermi

surface of the two groups, through the definition

$$\frac{\alpha}{1-\alpha}=\frac{N_1(\epsilon_{F1})}{N_2(\epsilon_{F2})}\equiv\left[\frac{\chi_{01}}{\gamma_1^2}\right]\left[\frac{\chi_{02}}{\gamma_2^2}\right]^{-1}. \tag{9}$$

The cross-scattering rates are then expressed in terms of α and a single parameter τ_x by the relations

$$\tau_{12}^{-1}=\alpha\tau_x^{-1},\quad \tau_{21}^{-1}=(1-\alpha)\tau_x^{-1}, \tag{10}$$

which will automatically satisfy the reciprocity relation equation (8). In the model, this intergroup scattering also relaxes the momentum as well as establishing communication between the spin dynamics of the two groups, and as a consequence it is convenient to introduce a modified momentum relaxation time for each group,

$$\frac{1}{\tau_1}=\frac{1}{\tau_1'}+\frac{1-\alpha}{\tau_x}, \tag{11a}$$

$$\frac{1}{\tau_2}=\frac{1}{\tau_2'}+\frac{\alpha}{\tau_x}. \tag{11b}$$

In the spirit of an almost-free-electron model for aluminum, in which the second- and third-zone surfaces are simply different pieces of a single free-electron spherical Fermi surface, it is plausible to assume the exchange interaction between any pair of electrons to be independent of whether they are in the same or different zones. In this approximation, $\zeta_{11}=\zeta_{22}=\zeta_{12}$, the B's may be expressed in terms of a single B_0 by

$$\begin{aligned}&B_{11}=B_{21}=\alpha B_0,\\&B_{12}=B_{22}=(1-\alpha)B_0.\end{aligned} \tag{12}$$

Finally, in the spirit of this same model, the partial susceptibilities, in absence of exchange, are conveniently written [see PW equation (53.26)] as

$$\chi_{0i}=\begin{bmatrix}\alpha\\1-\alpha\end{bmatrix}\gamma_i^2 mp/4\pi^2, \tag{13}$$

with m the electron mass and p the Fermi momentum in the free-electron model.

The transport equations, generalizations of PW equations (58.23) and (59.29), for the amplitudes a_i (magnetization) and $\vec{b}_i$ (magnetization current) are

$$\left[-i[\omega-\Omega_1(1+\alpha B_0)]+\frac{1+\alpha B_0}{T_1}+\frac{1-\alpha}{\tau}\right]a_1+\left[iB_0\Omega_1(1-\alpha)+\frac{B_0(1-\alpha)}{T_1}-\frac{1-\alpha}{\tau_x}\right]a_2+i\vec{k}\cdot\vec{b}_1/3=i\Omega_1\gamma_1 H_1, \tag{14a}$$

$$\left[-i(\omega-\Omega_1)+\frac{1}{\tau_1}+\frac{1-\alpha}{\tau_x}\right]\vec{b}_1+\vec{\omega}_{c1}\times\vec{b}_1+ikv_1^2[(1+\alpha B_0)a_1+(1-\alpha)B_0a_2]=0, \tag{14b}$$

and two additional equations being obtained from Eqs. (14a) and (14b) with the following transformations:

$$1\rightleftarrows 2$$

and

$$\alpha\rightleftarrows 1-\alpha.$$

The $\vec{\omega}_{ci}$ are vectors of magnitude equal to the cyclotron resonance frequency and direction parallel to $\vec{H}_0$. In these equations Ω_1 and Ω_2 are the single-electron resonance frequencies in the applied field plus exchange field of the other electrons [with the use of Eqs. (4) and (12)]:

$$\Omega_1=\gamma_1 H_0\frac{1+B_{22}-(\gamma_2/\gamma_1)B_{12}}{(1+B_{11})(1+B_{22})-B_{12}B_{21}}=\gamma_0 H_0\left|\frac{1-\epsilon}{1+\epsilon}\right|^{1/2}\left[1-\frac{2\epsilon(1-\alpha)B_0}{1-\epsilon}\right]\frac{1}{1+B_0}. \tag{15a}$$

Ω_2 is obtained from Eq. (15a) with

$$1\rightleftarrows 2,\ \alpha\rightleftarrows 1-\alpha,\ \epsilon\rightleftarrows-\epsilon. \tag{15b}$$

The prediction of experimental transmission-electron spin resonance (TESR) results requires the solution of Eqs. (14) with suitable boundary conditions on the amplitudes $a_i,\vec{b}_i$. In absence of surface-induced spin relaxation, the conventional boundary condition for a single species of mobile spins is simply $\hat{n}\cdot\vec{j}=0$ at a surface with outward normal $\hat{n}$. For the two-spin model, in the absence of surface relaxation, the same condition is appropriate for the total magnetization current, but not individually for the currents $\vec{j}_1$ and $\vec{j}_2$. An additional condition must be imposed which defines the extent to which the surface contributes to intergroup scattering, a process which will leave the normal components of the total magnetization current effectively zero, but which may allow the outward flow of magnetization in one electron group to be balanced by an inward flow in the other. Such scattering leads to quite complicated additional boundary conditions on the amplitudes $a_i,\vec{b}_i$ except in the special case of the static magnetic field oriented perpendicular to the surface. This special case is useful to develop in order to illustrate the possible consequences of spin-independent surface scattering.

The surface scattering is modeled as a "specular" fraction $(1-\beta)$ which takes $\vec{v}$ into $\vec{v}-2\hat{n}(\hat{n}\cdot\vec{v})$ in the same group, and a "diffuse" fraction β which

scatters randomly in direction and to final states in both groups 1 and 2 with relative weights α and $1-\alpha$. Assuming the deviation from equilibrium at the surface to have the simple form of Eq. (1), the spin-density flux at the surface associated with *out*ward moving electrons in group i is proportional to

$$J_{0i} \propto \begin{bmatrix} \alpha \\ 1-\alpha \end{bmatrix} \int_0^1 v_i \cos\theta (a_i + b_i v_i \cos\theta) d\cos\theta$$

$$\propto \begin{bmatrix} \alpha \\ 1-\alpha \end{bmatrix} (a_i v_i/2 + b_i v_i^2/3) . \tag{16a}$$

Similarly the *in*ward moving electrons give a spin-density flux

$$J_{Ii} \propto \begin{bmatrix} \alpha \\ 1-\alpha \end{bmatrix} (a_i v_i/2 - b_i v_i^2/3) . \tag{16b}$$

Setting the reflected flux (inward flux) equal to appropriate reflected amplitudes of the outward flux, e.g.,

$$\begin{aligned} J_{I1} &= J_{01}[(1-\beta)+\beta\alpha] + J_{02}\beta\alpha , \\ J_{I2} &= J_{01}\beta(1-\alpha) + J_{02}[(1-\beta)+\beta(1-\alpha)] , \end{aligned} \tag{17}$$

gives the boundary conditions for the amplitudes a_i and b_i. Assuming for simplicity that $v_1 = v_2 = v_F$, these become

$$\alpha b_1 + (1-\alpha) b_2 = 0 , \tag{18a}$$

$$\pm(b_2 - b_1) v_F = \tfrac{3}{2}\beta(a_2 - a_1)/(2-\beta) . \tag{18b}$$

The plus (minus) sign is appropriate if the outward normal to the surface is in the positive (negative) z direction; the b_i are the z components of the $\vec{b}_i$, the x and y components being zero for a geometry with the static field perpendicular to the surface. The boundary conditions (for $\beta \neq 0$) become much more complicated if the static field is not perpendicular to the surface. For the perpendicular geometry discussed here, Eq. (18a) is the direct generalization of the usual result $\hat{n} \cdot \vec{j} = 0$, while Eq. (18b) describes the intergroup scattering resulting from the diffuse fraction β. Note that for $\beta = 0$ these equations imply $b_1 = b_2 = 0$, i.e., the normal magnetization currents for both groups are individually zero; if $\beta \neq 0$ magnetization may be carried toward the surface by one group and returned into the bulk by the other, and the surface scattering effectively couples the two groups in a manner similar to the terms in τ_x^{-1}.

B. Poles of $\chi(k,\omega)$ as $k \to 0$

The simplest result to obtain is the susceptibility in the $k = 0$ limit. The real and imaginary parts of the poles of the susceptibility indicate the resonance frequencies and widths of the system response to a spatially uniform driving field, and give as well a general idea, with qualifications concerning surface-induced relaxation, of the TESR response in the "thin limit" in which the spin-diffusion length $\sim(v_F^2 \tau T)^{1/2}$ or spin-wave wavelength $|k|^{-1}$ is large compared with the sample thickness. In the $k = 0$ limit Eq. (14a) and its transformation for the magnetization decouple from Eq. (14b) and its transformation for the magnetization currents to give a relatively simple secular equation, quadratic in frequency, the roots of which are the poles of the $k = 0$ susceptibility. The dependence of the real and imaginary parts of these poles upon the cross relaxation time τ_x is discussed in Sec. III.

C. Dispersion relation $k^2(\omega)$

For $\vec{k} \neq 0$, spin diffusion or spin-wave propagation becomes important, and the exact solution of Eqs. (14) with the applied field perpendicular to a foil sample subject to the boundary conditions (18), though straightforward in principle, is tedious and would be useful only in making comparisons with specific experimental results. (The situation for the parallel field geometry is more complicated because of the greater complexity of the boundary conditions for this situation.) As a consequence of the two groups of electrons in the model there are two solutions of the homogeneous part of Eqs. (14) corresponding to spin diffusion or spin-wave propagation in two distinct modes. The general solution requires the determination of four mode amplitudes corresponding to the propagation of both modes in both the positive and negative directions across the sample. The diffuse boundary conditions (18), or their generalization for the parallel geometry, are important in giving mixing at the surfaces of the eigenmodes of the bulk material. Under the assumption of specular reflection ($\beta = 0$) at the surfaces, the solutions are relatively straightforward for arbitrary orientation, because of the absence of mode-mode coupling at the surface, but do in general require numerical analysis.

More instructive than attempting exact solutions is to examine the behavior of the model near the high-temperature limit, in the regions in which the cross-scattering rate $1/\tau_x$ is still large compared with the difference in frequencies associated with the g-value splitting. In this case one of the poles of the susceptibility has a relatively small imaginary part determined by a weighted mean of $1/T_1$ and $1/T_2$, while the other pole has an imaginary part the order of $1/\tau_x$. For the thick-sample problem, the transmission is dominated by a single mode, since

the propagating mode corresponding to the susceptibility pole with the large imaginary part is very heavily attenuated. It is reasonable then to solve Eqs. (14) in the limit of small τ_x to obtain the dispersion relation $k(\omega)$ for the dominant spin-diffusion model and to use this $k(\omega)$ in the standard formulas for TESR signal shapes.

The following equation [Eq. (19)] gives the dispersion relation, in a complete but not very useful form, to first order in the ratio of the TESR linewidth to the cross-scattering rate. Also terms higher than first order in the fractional g-value splitting ϵ, the exchange splitting B_0, and their product ϵB_0 have been deleted:

$$k^2=\frac{1}{(1+B_0)D_e}\left\{\left[-i\tilde{\omega}+\frac{1+B}{T_e}\right]-\tau_x\alpha(1-\alpha)\left\{-\tilde{\omega}^2(1-B_0)\left[\frac{D_2-D_1}{D_e}\right]^2\right.\right.$$
$$+\tilde{\omega}\frac{D_2-D_1}{D_e}\left[\frac{2i}{D_e}\left[\frac{D_1}{T_2}-\frac{D_2}{T_1}\right]-4\gamma_0H_0\epsilon\right]$$
$$\left.\left.+\frac{1+B_0}{D_e}\left[\frac{D_1}{T_2}-\frac{D_2}{T_1}\right]\left[\frac{1}{D_e}\left[\frac{D_1}{T_2}-\frac{D_2}{T_1}\right]+4i\gamma_0H_0\epsilon\right]\right\}\right\}. \tag{19}$$

Several new symbols require definition and comment: First,

$$\tilde{\omega}\equiv\omega-\gamma_0H_0[1+\epsilon(1-2\alpha)] \tag{20}$$

is the deviation, in first order in ϵ, of the applied frequency ω from the weighted average, $[\alpha\gamma_1+(1-\alpha)\gamma_2]H_0$, of the resonant frequencies, in absence of exchange, of the two individual groups; second,

$$1/T_e\equiv(\alpha/T_1)+(1-\alpha)/T_2 \tag{21}$$

is the corresponding weighted average of the individual linewidths; third, the D_1 and D_2 are anisotropic diffusion constants given by

$$D_i=\frac{v_i^2}{3}\frac{[-i(\omega-\Omega_i)+(1/\tau_i)]^2+\omega_{ci}^2\cos^2\Delta}{[-i(\omega-\Omega_i)+(1/\tau_i)]\{[-i(\omega-\Omega_i)+(1/\tau_i)]^2+\omega_{ci}^2\}} \tag{22}$$

with Δ the angle between the applied static field H_0 and the direction of the spin-wave or spin-diffusion wave vector k. Note that in the limit of short relaxation times $D_i\rightarrow v_i^2\tau_i/3$; D_e is a weighted diffusion constant,

$$D_e\equiv\alpha D_1+(1-\alpha)D_2\ . \tag{23}$$

The leading term of Eq. (19) is equivalent to the dispersion implied by PW equations (58.32) and (58.33) if ω in Eq. (22) is replaced by the ω_s of PW, a substitution made in their development which is appropriate for ω near the TESR resonance. The correction terms, to first order in τ_x, give the first effects of the decoupling of the two groups of spins as τ_x is increased, or temperature is decreased.

Equation (19) may be forced into the form

$$k^2=\frac{1}{D^*}\left[-i\tilde{\omega}^*+\frac{1}{T^*}\right] \tag{24}$$

by using the definitions

$$D^*=(1+B_0)D_e\left[1-\alpha(1-\alpha)\tau_x\left\{\frac{D_2-D_1}{D_e}\left[4i\epsilon(\gamma_0H_0)+\frac{2}{D_e}\left[\frac{D_1}{T_2}-\frac{D_2}{T_1}\right]\right]+i\tilde{\omega}(1-B_0)\left[\frac{D_2-D_1}{D_e}\right]^2\right\}\right], \tag{25}$$

$$\tilde{\omega}^* = \tilde{\omega} + 4\alpha(1-\alpha)\tau_x(1+B_0)(\gamma_0 H_0)\epsilon\left[\frac{1}{T_2}-\frac{1}{T_1}\right] \equiv \omega - \gamma^* H_0 \,, \tag{26}$$

$$\frac{1}{T^*} = \frac{1+B_0}{T_e} - \alpha(1-\alpha)\tau_x(1+B_0)\left[\frac{1}{T_2}-\frac{1}{T_1}\right]^2 . \tag{27}$$

This form is convenient for comparison with data analyzed on the basis of the PW result of the form of Eq. (24). The discussion of the next section reveals how the correction terms may contribute both to a g-value shift and a change in phase of the diffusion constant deduced from the TESR data. Note that these correction terms all depend, in one way or another, upon the difference between the properties γ_i, T_i, or D_i, of the two groups of electrons. Note that Eq. (27), because the expansions have been carried only to first order in ϵ, does *not* include the most important term linear in τ_x, a term quadratic in ϵ.

III. PREDICTIONS OF THE MODEL

A. Poles of the uniform susceptibility

In order to illustrate the complexities of the ESR response implied by this model, and hence the complexities which may be expected in the interpretation of TESR data in aluminum and presumably in other polyvalent metals as well, the trajectory of the poles of the uniform susceptibility $\chi(k=0,\omega)$ with varying temperature are plotted in Fig. 2. The secular equation derived from Eqs. (14) with $k=0$ is solved for a complex ω and the imaginary part of ω plotted

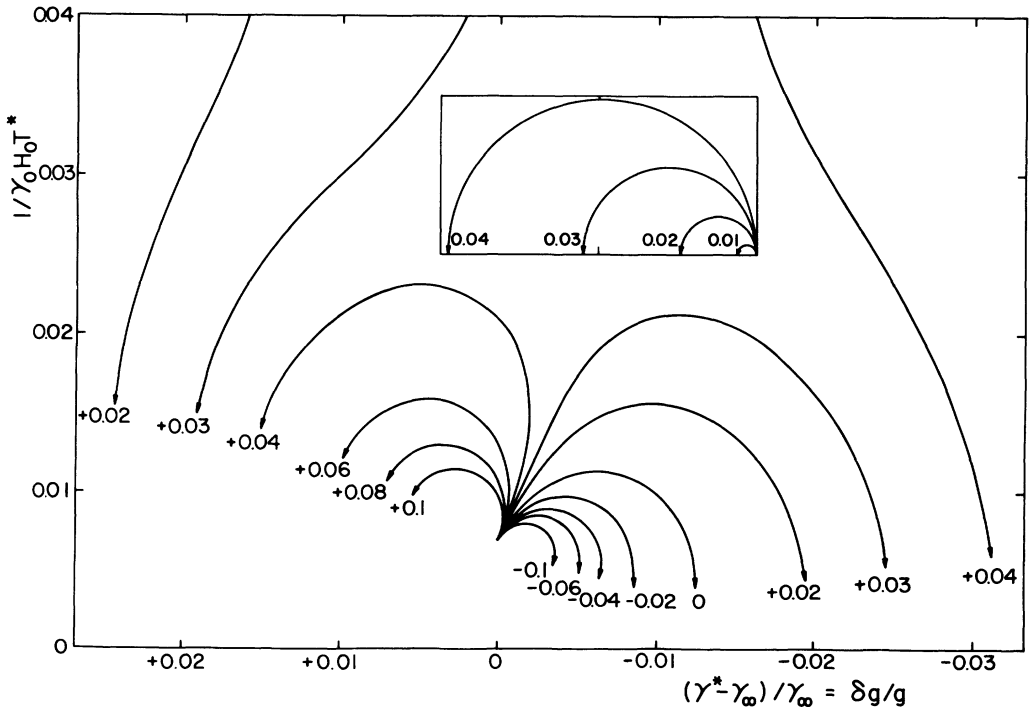

FIG. 2. Pole trajectories of $\chi(k=0,\omega)$ with the interzone relaxation rate $1/\tau_x$ as parameter. The point from which the various trajectories spread out is the high-temperature limit $\gamma_0 H_0 \epsilon \tau_x \ll 1$; the arrowheads are the low-temperature limits. The plotted trajectories are for the parameter values $\alpha=0.25$, $\epsilon=-0.025$, $\gamma_0 H_0 T_1=62.5$, $\gamma_0 H_0 T_2=250$. The labels on the individual trajectories give the B_0 values. These curves may also be used to determine the trajectories for $\epsilon=+0.025$ by reversing the signs on the B_0 labels and reversing the signs on the $\delta g/g=(\gamma^*-\gamma_\infty)/\gamma_\infty$ axis. The inset shows trajectories in the FF model for $B_0=+0.1$ and $\langle(\delta g/g)^2\rangle^{1/2}$ given by the labels on the curves; the scales are the same as in the main figure, but the origin is displaced.

against the real part as τ_x is varied to represent the effect of changing temperature. Other parameters are defined as $\alpha=0.25$, $\epsilon=-0.025$, $\gamma_0 H_0 T_2=250$, $\gamma_0 H_0 T_1=62.5$, and B_0 is assigned the values labeling the various curves. The vertical and horizontal scales give the linewidth and line shift in units of $\gamma_0 H_0$, or, if thought of as field rather than frequency, in units of the resonance field H_0. The line shifts are measured with respect to the high-temperature, motionally narrowed limit

$$\gamma_\infty=\gamma_0[(\alpha\gamma_1+(1-\alpha)\gamma_2] \ .$$

The shared point on these curves is the high-temperature limit, each curve showing the variation of the pole position as the temperature is lowered (the τ's made longer) to a low-temperature limiting value represented by the arrowhead. In addition to the set of trajectories which fan out from the high-temperature limit, there is a second set whose imaginary parts go to $1/\tau_x$ at high temperatures but which come to observable values at low temperatures. For $B_0=0$, the low-temperature limits are, of course, the individual $1/T_i$ and γ_i values in appropriate units for each of the two groups; for $B_0 \gg \epsilon$ the two roots become the collective mode and the exchange-shifted single-particle modes of FF.[2] The inset gives the trajectories in the FF model,

$$(\gamma^*-\gamma_\infty)/\gamma_\infty=\frac{B_0\langle(\delta g/g)^2\rangle(\gamma_0 H_0)^2\tau_x^2}{1+X^2} \ , \quad (28)$$

$$(\gamma_0 H_0 T^*)^{-1}=\frac{(1+B_0)\langle(\delta g/g)^2\rangle(\gamma_0 H_0)\tau_x}{1+X^2} \ , \quad (29)$$

$$X=[B_0/(1+B_0)](\gamma_0 H_0)\tau_x \ , \quad (30)$$

for $B_0=+0.1$ and several values of $\langle(\delta g/g)^2\rangle^{1/2}$. In Eq. (29) only the contribution of the narrowed g-value distribution is written. The results of Beuneu[7] give $\langle(\delta g/g)^2\rangle^{1/2}=0.033$, comparable with the value of 0.022 used in the results presented here.

Several features in Fig. 2 are worthy of note, and emphasize the need for care in the interpretation of TESR data for systems with exchange and g-value anisotropy of comparable magnitude:

(1) The two-spin model with no exchange can give a motional narrowing transition which simulates the FF transition; compare the main Fig. 2, with $B_0=0$, with the inset with $\langle(\delta g/g)^2\rangle^{1/2}\sim 0.032$ and suppose the horizontal axis of the main figure reversed to correspond to $\epsilon>0$.

(2) Similar g-value shift versus temperature curves may be simulated by a wide range of curves generated with different values of the parameter pair B_0,ϵ. For example, $\epsilon=-0.025$, $B_0=+0.07$ is roughly simulated by $\epsilon=+0.025$, $B_0=+0.02$. (Again recall, for $\epsilon=0.025$, to reverse the sign of the $\delta g/g$ axis, and to reverse the signs of the B_0 labels.)

(3) The two-spin model, with unequal relaxation times T_i, can show a nonmonotonic variation of resonance position with temperature, in contrast to the simple motional narrowing model and the FF model in both of which the g-value shift is monotonic. In the example of Fig. 2 this behavior is revealed for B_0 and ϵ of opposite sign and roughly $|B_0|>|\epsilon|$.

(4) The two-spin model, obviously, reveals the possibility of observing a two-line structure related to the g-value anisotropy in the case of weak exchange in the low-temperature limit. Note that in this case the weak exchange may shift the resonances substantially from the positions determined by the γ_i's in the absence of exchange; compare, for example, the low-temperature limits for the narrower pole (i.e., smaller imaginary part) in Fig. 2 for $B_0=\pm 0.02$ with the limit for $B_0=0$. This same shift has brought the broader ($i=1$) pole from off scale to the left of the figure, for $B_0=0$, onto the graph for $B_0=+0.02$.

With the information on $\delta g(\vec{k})$ provided by Beuneu, and the observations above suggested by the two-spin model, it is amusing (though not very productive it turns out) to speculate about the interpretation of the high-frequency TESR data of Dunifer *et al.*[6,8] Dunifer's data,[6] as well as many other results,[5,13] *do* show a nonmonotonic variation of g with temperature, suggestive of point (3) above, and it is tempting to conclude that B_0 and ϵ have opposite sign. It would be difficult, however, to rule out all of the other possibilities outlined by Beuneu[7] for the increasing g at higher temperatures and the conclusion must remain tentative. It does suggest that the crystal-field matrix element V_{111}, whose sign is dominant in determining the sign of ϵ, may turn out to be negative rather than positive as is generally assumed.

Considerations (1) and (2) suggest ambiguities in the procedures for deducing B_0 values from the TESR data for aluminum; certainly the magnitude and conceivably the sign of B_0 as determined from an FF analysis of results on thin samples could be in error, and there might even be a possibility of approximating the low-temperature shifts with g-value anisotropy without exchange. This suggests the need for reexamination, in the framework of this model, of the interpretation of higher-temperature data on thicker samples which have served as the basis of B_0 determinations for aluminum.[8]

In a speculative frame of mind one could imagine an interpretation of the spin-wave spectrum of Fig. 5 of Ref. 8 as being due to a pair of resonance

modes, one from each of two decoupled groups of spins with the broader and weaker resonance having a larger g value (lower resonance field). The splitting suggested by the data would be $\Delta H/H \sim 0.025$, about half of that calculated by Beuneu[7] but close enough to be interesting. Although the results of Ref. 14 confirm the spin-wave interpretation, the suggestion illustrates the potential ambiguity. This ambiguity is most straightforwardly removed by comparing results in the parallel and perpendicular field geometries, since the spin-wave structure will appear on opposite sides of the main line for the two geometries, while structure induced by g-value anisotropy will be insensitive to sample orientation.

In view of these qualitative remarks we ask, is it worthwhile to pursue the development of the model in order to attempt quantitative fits to Dunifer's[6] results? The answer is probably no. The most remarkable feature of the data is the unexplained decrease in linewidth with sample thickness, discussed by them at some length. The remarks above shed no light on this behavior, though a brief relevant comment will appear in the next section. Without even a qualitative understanding of the linewidth variation with thickness, any attempt at a quantitative understanding of the line shifts seems pointless. The linewidth variation is further obscured by the onset of phonon broadening for $T \gtrsim 35$ K, preventing linewidth versus g-value shift comparisons in the interesting regime in which the g value is increasing with increasing temperature. Finally, the two-spin model both is so inadequate in some regards, e.g., the phenomenological inclusion of the T_i^{-1} which themselves are likely to be "Freedman-Fredkin widths," and contains so many adjustable parameters, that any quantitative agreement would be of doubtful significance.

B. Response at finite wave vector

As noted in Sec. II, the solution of Eq. (14) for any except "specular," $\beta=0$, boundary conditions is expected to be very tedious, and indeed for the parallel field geometry the appropriate boundary conditions are unclear. An important feature to note, however, is that the surface scattering, if $\beta \neq 0$, mixes the two groups of electrons 1 and 2. For a thin sample this mixing plays the same role as τ_x and can be incorporated by an adjusted value for τ_x. The thick case is different, however. The normal modes of propagation involve a mixture of the electron groups 1 and 2 with coefficients determined by the various model parameters including the bulk scattering τ_x. Typically, one of the two modes is strongly attenuated with distance into the sample, and the other dominates the TESR signal. The surface scattering now scatters electrons from the weakly attenuated mode to the strongly attenuated mode and consequently has the effect of a surface spin relaxation for the better propagating mode. Surface scattering between the modes, even though not involving a spin flip, has the effect of a surface spin relaxation. In the FF language, the collective spin mode is damped at the surface by surface scattering between it and the single-particle modes. The effectiveness of this surface relaxation depends, through the mode admixture coefficients, in a complicated way upon the model parameters. It is possible that the increase in width with decreasing sample thickness observed by Dunifer and Pattison[6] is related to this intermode surface scattering; no attempt has been made to pursue this idea quantitatively.

An alternative to studying the low-temperature, $(\epsilon,B_0)\gamma_0 H_0 \tau_x > 1$, behavior of this model is to look at the first-order corrections in leaving the high-temperature, $(\epsilon,B_0)\gamma_0 H_0 \tau_x \ll 1$, regime. The results in this regime depend less upon specific details of the model and are more useful in addressing questions such as the reliability of B_0 determinations from TESR data.

The expression of Eq. (19), and consequently of Eqs. (25)–(27), may be simplified considerably if one is interested only in the rough magnitudes of the first-order corrections in τ_x. Suppose in the regime of interest, temperatures below the observed linewidth minimum, that the linewidths T_i^{-1} of the two groups are determined by motional or exchange narrowing of the g-value anisotropy within each of the individual zones. The results of Beuneu[7] suggest taking $T_1^{-1}/T_2^{-1} \sim \langle \delta g^2 \rangle$ (third zone)/$\langle \delta g^2 \rangle$ (second zone) ~ 9, or for the purposes of this discussion, simply $1/T_1 \gg 1/T_2$. The results of Ref. 15 imply scattering rates for third-zone electrons roughly $10\times$ faster than for second-zone electrons, and hence that in the regime $\omega_c \tau \ll 1$, the electron transport is dominated by the second-zone electrons, $D_2 \gg D_1$. Further, because the cyclotron resonance frequency for the third-zone electrons is the order of $10\times$ higher than the second zone, the condition $D_2 \gg D_1$ is also appropriate in the regime $\omega_c \tau \gg 1$ for the parallel field geometry. With these approximations, $1/T_1 \gg 1/T_2$ and $D_2 \gg D_1$, Eqs. (25)–(27) become

$$D^* = (1+B_0)(1-\alpha) \times D_2 \left[1-\alpha\tau_x \left[4i\epsilon\gamma_0 H_0 - \frac{2}{\alpha(1-\alpha)T_e} + \frac{i\tilde{\omega}(1-B_0)}{(1-\alpha)} \right] \right], \quad (31)$$

$$\tilde{\omega}^* = \tilde{\omega} - 4(1-\alpha)(1+B_0)(\gamma_0 H_0)\epsilon\tau_x \frac{1}{T_e} , \quad (32)$$

$$\frac{1}{T^*} = \frac{1+B_0}{T_e}\left[1 - \frac{1-\alpha}{\alpha}\frac{\tau_x}{T_e}\right] . \quad (33)$$

Note again that the dominant (FF) correction to $1/T^*$, of order $\epsilon^2(\gamma_0 H_0)^2\tau_x$ [see Eq. (29)], does not appear in this result, which is carried to only first order in ϵ.

Analysis of CESR data is conveniently performed by fitting experimental line shapes to the PW theory which uses the dispersion relation Eq. (24), with D^* given by PW equation (58.33), T^* by the T_2 of PW, and $\tilde{\omega}^*$ by the $\omega - \omega_s$ of PW. The implications of the two-spin model are then summarized by comparing the D^*, $\tilde{\omega}^*$, and T^* given above with the corresponding PW results.

The most important implication of this model is for the complex diffusion constant D^*, and in particular for the exchange parameter deduced from the temperature dependence of D^*. Equation (31) gives three correction terms as the cross-scattering rate τ_x^{-1} becomes weak. The last, involving $\tilde{\omega}$, is zero on resonance and represents a correction to the line shape predicted by the PW theory, but a correction which becomes important only in the wings of the line. Since this analysis, the hydrodynamic limit, is suspect[16] in any case in the wings of the line, this term is ignored. The second term is principally a small and experimentally unobservable correction to the real part of the diffusion constant. The first term, however, influences significantly the ratio of the real to imaginary parts of the diffusion constant and must be considered further. To examine its influence Eq. (22) for D_2 is first evaluated, in the limit $(\gamma_0 H_0)\tau_x B_0 \ll 1$, and the ratio of imaginary to real parts is calculated to be

$$R_2 \equiv \mathrm{Im}D_2/\mathrm{Re}D_2 = (\gamma_0 H_0)\tau_2(B_0 - 2\alpha\epsilon) \times \left[1 - \frac{2}{1+\omega_{c2}^2\tau_2^2\cos^2\Delta} + \frac{2}{1+\omega_{c2}^2\tau_2^2}\right] , \quad (34)$$

the term in $\alpha\epsilon$ being analogous to the result of Kaplan and Glasser.[3] In this result terms of higher than first order in B_0 and ϵ have been neglected as well as terms in ϵB_0. Combining Eqs. (34) and (31) gives for the two-spin model

$$R^* \equiv \mathrm{Im}D^*/\mathrm{Re}D^* = (\gamma_0 H_0)\left[-4\epsilon\alpha\tau_x + (B_0 - 2\alpha\epsilon)\tau_2\left[1 - \frac{2}{1+\omega_{c2}^2\tau_2^2\cos^2\Delta} + \frac{2}{1+\omega_{c2}^2\tau_2^2}\right]\right] . \quad (35)$$

For a single spin species, the corresponding PW result is simply

$$R_{\mathrm{PW}} = (\gamma_0 H_0)\tau B_0\left[1 - \frac{2}{1+\omega_c^2\tau^2\cos^2\Delta} + \frac{2}{1+\omega_c^2\tau^2}\right] . \quad (36)$$

The expression in the large parentheses of each of these equations describes the dependence of the ratio R upon the magnetic field orientation relative to the plane of the sample and is $+1$ for the perpendicular field configuration and $(1-\omega_c^2\tau^2)/(1+\omega_c^2\tau^2)$ for the parallel field.

There are three important consequences of these results. Suppose the data taken in a perpendicular field geometry are analyzed using the PW model and Eq. (36) is used to deduce an "experimental" value of B_0 which will be denoted $B_\perp$. Comparison of Eqs. (35) and (36) shows that the two-spin model would imply a value for B_0,

$$B_0 = B_\perp + 2\alpha\epsilon(1 + 2\tau_x/\tau_2) . \quad (37)$$

Noting that $\alpha = \frac{1}{4}$ is appropriate for aluminum,[7] and recalling Eq. (11b), the correction may be expressed as

$$|B_0 - B_\perp| > \tfrac{3}{4}|\epsilon| \simeq 0.02 , \quad (38)$$

a sizable correction in view of the measured value[8] of $0.05 < B_0 < 0.2$. Here ϵ is taken from Beuneu[7] to be ± 0.025.

In principle, the consequences of the two-spin groups and g-value anisotropy can be separated from the exchange effects, within the framework of this model, by comparing the data taken in parallel and perpendicular orientations, since for parallel field the result analogous to Eq. (37) is

$$B_0 = B_{||} + 2\alpha\epsilon\left[1 - \frac{2(\tau_x/\tau_2)(\omega_{c2}^2\tau_2^2+1)}{\omega_{c2}^2\tau_2^2 - 1}\right] . \quad (39)$$

In the large-$\omega_c\tau$ limit, the effect of the incipient spin wave is to give the opposite sign to R_{PW} for parallel and perpendicular fields while the major effect of the g-value splitting is orientation independent. Equations (37) and (39) combine to give the result

$$B_{||}-B_{\perp}=8\alpha\epsilon\frac{\tau_x}{\tau_2}\frac{\omega_{c2}^2\tau_2^2}{\omega_{c2}^2\tau_2^2-1} \tag{40a}$$

and, in the limit $\omega_c\tau\gg 1$,

$$|B_{||}-B_{\perp}|=8\alpha|\epsilon|\tau_x/\tau_2\geq 8\alpha^2|\epsilon|\ , \tag{40b}$$

with the inequality based on Eq. (11b). The model predicts then, using $\alpha=\frac{1}{4}$ and $\epsilon=\pm 0.025$, a discrepancy of at least 0.012 in the value of B_0 determined from a PW analysis of data taken with field perpendicular and parallel when in the limit $\omega_c\tau\gg 1$. The sign of the discrepancy gives the sign of ϵ and hence, via the g-value calculation,[7] the sign of the matrix element V_{111}.

A second important consequence of the model concerns the magnitude of the diffusion constant D^*. In the analysis of TESR data, a principal ambiguity in determining B_0 is the determination of τ since [see Eq. (36)] it is the product $B_0\tau$ which is effectively accessible to measurement. In the PW model, with ω_c and v_F assumed known, τ may be determined either from the behavior with temperature of the diffusion constant for the field parallel to the sample, which reaches a maximum at $\omega_c\tau=1$ and has the behavior expressed by Eq. (22) as a function of $\omega_c\tau$, or from the magnitude of the diffusion constant for a perpendicular field, $D=v_F^2\tau(1+B_0)/3$.

In a system, such as aluminum, with a complex Fermi surface the situation is of course not so simple; in the two-spin model the magnitude of the apparent diffusion constant and its $\omega_c\tau$ dependence must be worked out from the most intractable set of Eqs. (22), (23) and (25). If one can argue that the electron transport is dominated by a single group of electrons, then the equations again become tractable. In aluminum it is the second-zone electrons that contribute principally to the spin diffusion,[15] both for small $\omega_c\tau$ and large $\omega_c\tau$; hence the temperature dependence of the signal in the parallel geometry is determined by $\omega_{c2}\tau_2$. However, Eq. (23) implies $D_e\approx(1-\alpha)D_2$, a reduced diffusivity, because only a limited fraction of the electrons contribute to the transport. For $\alpha=\frac{1}{4}$, appropriate to aluminum,[7] the correction to the simple result $v_F^2\tau/3$ for the diffusion constant is only a factor of $\frac{3}{4}$, but could be much more dramatic in a situation in which the transport is dominated by the group with the lower susceptibility. (The extreme example is of course the case of the analogous problem of the coupled system of conduction electrons and local moments in which one species, often the one dominating the susceptibility, is completely immobile.) A consistent determination of B_0 from both the argument involving $\omega_c\tau$ and the relation $D\sim v_F^2\tau/3$ requires clear recognition of relative contributions of the electron groups to the transport. A final consequence is that Eq. (32) predicts a g-value shift with increasing τ_x, hence decreasing temperature, which is, of course, the term giving the leading correction to the high-temperature, fully narrowed result and which describes the horizontal component of the beginning of the trajectories illustrated in Fig. 2.

IV. CONCLUSIONS

The conduction spin resonance of polyvalent metals, for which there are several disjoint pieces of the Fermi surface, may show new features not predicted by existing descriptions of the effects of g-value anisotropy and exchange. A model is explored which treats the spin dynamics of two groups of electrons, with different g values, which are coupled by both momentum scattering and exchange. The theory of PW is generalized to describe this situation and some of the consequences are discussed.

In absence of exchange the model predicts g-value shifts with reduced temperature resulting from the decoupling of the two groups of spins, shifts which are similar in behavior, but different in mechanism, from those predicted by FF. In the limit of low temperature, the resonance may show structure as a consequence of the g-value splitting.

In the presence of exchange the model suggests a substantial correction to the predicted g-value shift of the FF theory as the dispersion in g values becomes comparable to the Landau parameter B_0. The sign of this correction depends upon the relative sign of B_0 and parameters describing the asymmetry of the g-value distribution.

At temperatures above those at which spin waves are clearly resolvable, the exchange parameter B_0 induces marked asymmetry in the line shapes of TESR lines for thick samples. Similar asymmetry may be produced by g-value anisotropy in the absence of exchange. A separation of the two effects may be achieved by comparison of results obtained in both the field-parallel and field-perpendicular geometries, and such an analysis is required to obtain an accurate measure of B_0 in the presence of substantial g-value anisotropy.

The presence of two electron groups introduces a further ambiguity in the interpretation of data intended to yield experimental values of B_0; in particular the τ deduced from the temperature variation of the electron diffusion for the field-parallel geometry, through $\omega_c\tau$, may be different from that deduced from the specific magnitude of the diffusion constant in perpendicular geometry, $D_{\perp}=v_F^2\tau/3$, if a single group model is adopted. A reliable value of τ

is required for the determination of B_0. The model gives a rough procedure for correcting for this ambiguity.

In many metals spin relaxation at the surfaces is unimportant relative to bulk relaxation except in very thin samples. In the two-spin model it is noted that, in the experimental regime of "thick" samples, surface scattering from one electron group to the other without spin flip can simulate surface spin relaxation since it transfers excitation from a weakly attenuated mode which dominates the TESR signal into a heavily damped mode.

With specific reference to aluminum it is noted that the sign of the g-value splitting parameter, ϵ in the model presented here, is determined by the sign of the pseudopotential matrix element V_{111}. In principle, the TESR results give information about this sign. First, the experimental g-value variation with temperature is importantly influenced by the relative sign of B_0 and ϵ; unfortunately this variation may be masked by other physical effects noted by Beuneu.[7] Second, there are predicted variations in line shapes resulting from the interference of the effects due to a g-value splitting with exchange effects. Such variations should be observable in the $\omega_c\tau > 1$ regime by comparison of results with the applied field parallel and perpendicular to the sample. Finally, the model should not be taken as a realistic representation of the physics in a real metal, but simply as a means to explore possible complications in real systems in which the g-value anisotropy is sufficiently large to make suspect an FF analysis.

ACKNOWLEDGMENTS

This work was supported by the National Science Foundation through Grant No. DMR-80-08546. Additional support, through the Cornell University Materials Science Center (Report No. 4703), is also acknowledged.

[1]R. Dupree and B. W. Holland, Phys. Status Solidi 24, 275 (1967).

[2]R. Freedman and D. R. Fredkin, Phys. Rev. B 11, 4847 (1975); D. R. Fredkin and R. Freedman, Phys. Rev. Lett. 29, 1390 (1972).

[3]J. I. Kaplan and M. L. Glasser, Phys. Rev. 183, 408 (1969).

[4]M. B. Walker, Phys. Rev. Lett. 33, 406 (1974); Can. J. Phys. 53, 165 (1975); D. S. Montgomery, J. Phys. F 11, 711 (1981).

[5]D. Lubzens, M. R. Shanabarger, and S. Schultz, Phys. Rev. Lett. 29, 1387 (1972); D. Lubzens and S. Schultz, *ibid.* 36, 1104 (1976).

[6]G. L. Dunifer and M. R. Pattison, Phys. Rev. B 14, 945 (1976).

[7]F. Beuneu, J. Phys. F 10, 2875 (1980); F. Beuneu, Ph. D. thesis, Université de Paris—Sud, 1979 (unpublished).

[8]G. L. Dunifer, M. R. Pattison, and T. M. Hsu, Phys. Rev. B 15, 315 (1977).

[9]R. H. Silsbee and F. Beuneu, Phys. Rev. B 27, 2682 (1983).

[10]N. W. Ashcroft, Philos. Mag. 8, 2055 (1963).

[11]A. Stesmans and J. Witters, Phys. Rev. B 23, 3159 (1981).

[12]P. M. Platzman and P. A. Wolff, Phys. Rev. Lett. 18, 280 (1967); detailed reference is made to the presentation in P. M. Platzman and P. A. Wolff, *Waves and Interactions in Solid States Plasmas,* Supplement 13 of *Solid State Physics* (Academic, New York, 1973).

[13]L. Janssens, A. Stesmans, J. Cousins, and J. Witters, Phys. Status Solidi B 67, 231 (1975); J. R. Sambles, G. Sharp-Dent, J. E. Cousins, A. Stesmans, and J. Witters, *ibid.* 79, 645 (1977); J. Van Meijel, A. Stesmans, and J. Witters, Solid State Commun. 21, 753 (1977); A. Stesmans and J. Witters, Phys. Rev. B 15, 4126 (1977).

[14]J. P. Long and R. H. Silsbee (unpublished).

[15]A. B. Meador and W. E. Lawrence, Phys. Rev. B 15, 1850 (1977); T. Wegehaupt and R. E. Doezema, *ibid.* 18, 742 (1978).

[16]A. R. Wilson and D. R Fredkin, Phys. Rev. B 2, 4656 (1970).